PERGAMON

International Journal of Solids and Structures 38 (2001) 3549–3562

INTERNATIONAL JOURNAL OF SOLIDS and STRUCTURES

www.elsevier.com/locate/ijsolstr

Strain rate effects on the thermomechanical behavior of polymers

Zhouhua Li, John Lambros *

Department of Mechanical Engineering, University of Delaware, Newark, DE 19716, USA

Received 12 December 1999; in revised form 15 May 2000

Abstract

The thermomechanical behavior of two common polymers, polymethyl methacrylate (PMMA) and polycarbonate (PC), subjected to compressive dynamic loading was investigated in this study. The stress–strain response of each material was examined, over a wide range of strain rates (10^{-4} to 10^{3} s^{-1}), using an Instron machine and a split Hopkinson pressure bar (SHPB). It was found that the compressive yield stress for both materials increases with strain rate increases. For PMMA, the material changes its compression behavior from ductile to brittle as strain rate increases. In the SHPB experiments, simultaneously to stress and strain measurements from the bars, temperature change was monitored using a high speed infrared HgCdTe detector array. The amount of plastic work converted to heat, β, was measured. For PC, this value was found to be within the range of 0.5 to 0.6. It was found that competition between thermal softening and strain hardening dictates the behavior of this material after yielding, in a process similar to that occurring in metals. For PMMA, a value of β could not be defined, because of the brittle nature of the material. However, some heating was observed during the failure of the PMMA specimen, suggesting that the material at this strain rate is not perfectly brittle.

Keywords: Polymers; Strain rate sensitivity; Thermomechanical coupling; Infrared detectors; Dynamic load; SHPB

1. Introduction

It is well known that plastic work in metallic and polymeric materials is dissipated as heat. The problem of how much of the plastic work is converted into heat has been under investigation for many years. A large volume of research on this topic has concentrated on metals (Farren and Taylor, 1925; Taylor and Quinney, 1934; Mason et al., 1994; Hodowany et al., 2000; Kapoor and Nemat-Nasser, 1998). For metallic materials conflicting values of the amount of plastic work converted into heat, usually denoted as β, have been reported in the literature. Initial work in this area, dating back as early as the 1920's, by Farren and Taylor (1925) and Taylor and Quinney (1934) showed that 90–95% of the energy expended in plastic deformation of a metal is converted into heat. More recently, in the work of Mason et al. (1994) and

* Corresponding author. Present address: Department of Aeronautical & Astronautical Engineering, Room 310 Talbot Lab, 104 South Wright Street, MC 236, Urbana, IL 61801, USA. Tel.: +1-217-333-2242; fax: +1-217-244-0720.

E-mail address: lambros@aae.uiuc.edu (J. Lambros).

0020-7683/01/$ - see front matter
PII: S0020-7683(00)00223-7

Hodowany et al. (2000), the dependence of β on plastic strain and strain rate for different metals was investigated. They found a variation of β from 60% to 90%, depending on the metal, strain and strain rate. In contrast, in the study of Kapoor and Nemat-Nasser (1998), a value of β approximately 100% for all the metals tested was found.

In contrast to metallic materials, limited work has been done on the determination of β for polymers. However, strain rate effects on purely mechanical behavior of polymers has been a focus of some studies. For example, Walley et al. (1989) studied rate sensitivity behavior of a number of polymers over the range of strain rates from 10^{-4} to 10^{3} s^{-1}. They found that all the polymers tested showed higher yield stress at high strain rate. They further speculated that adiabatic heating may be the reason for the drop in yield stress in some cases.

The first attempt at measuring temperature increase during mechanical deformation of polymers was made by Chou et al. (1973). In their work four different polymers were tested, also within the same range of strain rates as above. Temperature rise developed during deformation was measured using a thermocouple. One of their conclusions was that at high strain rates ($\sim$50 s^{-1}) mechanical work was completely converted into heat after a certain level of strain had been attained, i.e., when relaxation mechanisms and plastic flow start taking place. During the investigation of cold drawing process of polycarbonate (PC), Adams and Farris (1988) performed a series of tests at low strain rates (from 0.18 to 1.8 min^{-1}) and studied the energy conversion between mechanical work, heat and internal energy using deformation calorimetry. They found that during this non-adiabatic procedure 50–80% of the mechanical work was dissipated into the environment as heat, and the rest was stored as internal energy in the material. Boyce et al. (1992, 1994) and Arruda et al. (1995) have also investigated thermomechanical coupling in polymers. In their studies, polymethyl methacrylate (PMMA) was tested over a range of low strain rates, from 0.001–0.1 s^{-1}. Temperature change was monitored through a single unfocused infrared detector element. They found that the temperature increase during the test can cause thermal softening, and thus have a dramatic effect on the stress–strain behavior.

The importance of dynamic strain rate on heat generation in polymers has recently received renewed attention. Trojanowski et al. (1997) experimentally investigated heat generation in an epoxy resin, at strain rate of approximately 2500 s^{-1}, using a split Hopkinson pressure bar (SHPB) and a single-element infrared detector. (This procedure is similar to that used in the present study.) A significant temperature rise of 40°C was recorded for this material at this rate. Rittel (1999) also conducted a study of heat generation during high rate deformation of PC. He used the SHPB to provide loading and embedded thermocouples to provide transient temperature sensing. Values of β ranging from 0.4 to 1.0 were reported for strain rates from 5000–8500 s^{-1}. This quantity was also observed to be strain and strain rate dependent.

In the present study, heat generation during dynamic deformation of a nominally ductile polymer, PC, and a nominally brittle one, PMMA, is investigated. Dynamic loading is provided using a SHPB. Temperature on the specimen surface is monitored in real time using a focused high speed infrared detector array. Temperature is recorded at various points along the specimen length to allow for investigation of thermal homogeneity in the specimen. Mechanical homogeneity is investigated using the traditional SHPB signals.

2. Theoretical background

For an elastic–plastic, isotropic, homogeneous material, the heat conduction equation can be written as

$$\kappa\nabla^2 T - \rho c_p \dot{T} = \alpha(3\lambda + 2\mu) T \dot{\varepsilon}^{e}_{kk} - \beta\sigma_{ij}\dot{\varepsilon}^{p}_{ij}, \tag{1}$$

where κ is the thermal conductivity; T, the absolute temperature; c_p, the specific heat; α, the coefficient of thermal expansion; λ and μ, the elastic constants; σ_{ij}, ε^{e}_{ij} and ε^{p}_{ij} the stress, elastic strain and plastic strain

components, respectively, and β, the fraction of plastic work rate converted into heat. A dot denotes differentiation with respect to time.

In the case of dynamic loading, where adiabatic conditions usually prevail since the heat dissipates at a rate much slower than it is generated, Eq. (1) reduces to

$$\beta\sigma_{ij}\dot{\varepsilon}^{\mathrm{p}}_{ij} = \rho c_p \dot{T}. \tag{2}$$

In the above equation, the thermoelastic heating effect $\alpha(3\lambda + 2\mu)T\dot{\varepsilon}^{\mathrm{e}}_{kk}$ has been ignored since it is usually small compared to the contribution from the plastic work. From Eq. (2), it can be seen that the quantity β plays an important role in the generation of heat during dynamic loading. Quantity β can be written as

$$\beta_{\mathrm{diff}} = \frac{\rho c_p \dot{T}}{\dot{W}^{\mathrm{p}}}, \tag{3}$$

where the subscript diff denotes it is in differential form and the plastic work rate $\dot{W}^{\mathrm{p}}$ is given by $\dot{W}^{\mathrm{p}} = \sigma_{ij}\dot{\varepsilon}^{\mathrm{p}}_{ij}$. Rittel (1999) points out that in addition to this differential form of β, an alternative integral form may also be used. It is expressed as

$$\beta_{\mathrm{int}} = \frac{\int_0^t \rho c_p \dot{T}\,\mathrm{d}t}{\int_0^t \dot{W}^{\mathrm{p}}\,\mathrm{d}t}. \tag{4}$$

The integral form denotes a cumulative, as opposed to instantaneous, conversion of plastic work to heat up till time t in the deformation. The rate of conversion of mechanical work into heat, β, can be determined experimentally by simultaneous measurement of stress strain and temperature (Mason et al., 1994; Hodowany et al., 2000; Rittel, 1999).

3. Experimental setup

3.1. Materials

The materials used in this study were extruded PC from Sheffield plastics under the brand name of Hyzod and extruded PMMA from PolyCast Technology Corporation under the brand name of PolyCast. The specimens were cylindrical, with a length of 8 mm and a diameter of 6.35 mm. They were cut using a precision diamond saw from rod stock materials and their ends were polished to ensure they were parallel and flat. The cutting procedure was very slow and was accompanied by specimen cooling to avoid the introduction of machining heat-induced anisotropy in the specimen.

3.2. Experimental devices

Quasi-static tests were performed using an Instron screw-driven testing machine. During the test, grease was applied to both ends of the specimen to reduce friction and prevent barreling. Stress–strain curves were obtained from load-displacement measurements with compensation for machine compliance taken into account. All quasi-static tests were performed at room temperature and no attempt was made to measure the temperature change within the specimen during the quasi-static tests.

Dynamic loading was realized using a SHPB (Fig. 1). The incident $\varepsilon_{\mathrm{i}}(t)$, reflected $\varepsilon_{\mathrm{r}}(t)$ and transmitted $\varepsilon_{\mathrm{t}}(t)$ signals recorded by strain gauges on the SHPB were used to obtain the average stress and strain in a homogenously deforming specimen as follows (Follansbee, 1985):

$$\sigma(t) = \frac{AE\varepsilon_{\mathrm{t}}(t)}{A_{\mathrm{s}}}, \tag{5}$$

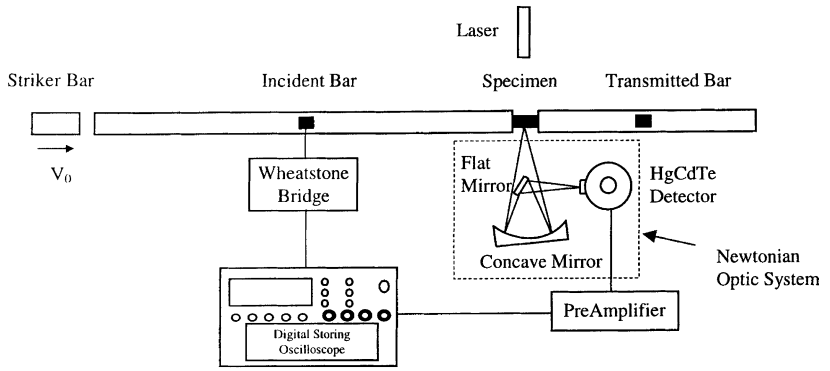

Fig. 1. SHPB and IR detector system.

$$\varepsilon(t) = \int_0^t -\frac{2c\varepsilon_r(\tau)}{L_s}\mathrm{d}\tau, \tag{6}$$

where A, E and c represent the cross-sectional area, Young's modulus and wave speed, of the bar respectively. L_s and A_s denote the length and cross-sectional area of the specimen. Details of the operation of the SHPB can be found in Follansbee (1985) and will not be discussed here. The data analysis procedure used for these experiments was discussed by Li and Lambros (1999). It includes both an experimental verification of homogeneous deformation (especially important when analyzing materials with low failure strains), and a dispersion correction for all signals recorded by the incident and transmitted strain gauges.

Real time transient temperature measurement is performed using a high speed infrared (IR) radiation detector array. The experimental setup used in the present study is similar to that used in Hodowany et al. (2000) and is also shown in Fig. 1. The IR detector array is a 16 element HgCdTe (mercury cadmium telluride) photovoltaic photon detector, custom made by Fermionics Inc. for this application. The size of each detector is 80 μm×80 μm, and the 16 detectors are arranged in a linear array with a center to center spacing of 100 μm, giving a total recording distance of 1.6 mm. For the HgCdTe elements used, the maximum responsivity covers wavelengths of 8–12 μm, which correspond to a black body temperature between 300–400 K (Zehnder and Rosakis, 1993), i.e. the range expected in our experiments. The detectors and related electronics have a signal rise time of approximately 250 ns, thus, providing sufficient temporal resolution to capture the transient temperature signals expected. The temperature resolution of the array (as will be seen subsequently) is of the order of 0.1 K, depending on the material tested. To obtain such a resolution the signal to noise ratio for the HgCdTe elements must be maximized. This is done by placing the detectors in a 77 K liquid nitrogen bath. Note that in contrast to the embedded thermocouple method (Rittel, 1999), this technique provides surface temperature only. However, it does offer higher temporal and spatial resolution, as well as the ability to obtain temperature at 16 locations on the specimen simultaneously (and thus experimentally investigate thermomechanical homogeneity).

The detector array is held stationary in front of the specimen and is focused onto the specimen surface. To allow for variable magnification a Newtonian focusing system is used. This consists of a concave and a flat mirror positioned as shown in Fig. 1. Both mirrors were gold coated to enhance reflectivity of infrared radiation. In the present experimentation, a magnification of one was used. The two detectors furthest apart, numbers 1 and 16, were used in this study in order to obtain measurements at discrete points on the specimen a length 1.6 mm apart. Monitoring the temperature at two points this far apart will allow for an additional experimental verification of homogeneous conditions during specimen deformation.

4. Mechanical response

Quasi-static tests on the Instron machine were carried out at two different strain rates, $\dot{\varepsilon} = 4 \times 10^{-5}$ s^{-1} and $\dot{\varepsilon} = 4 \times 10^{-2}$ s^{-1}. Stress–strain curves for PMMA and PC at both these two rates are shown in Figs. 2 and 3, respectively. Both PMMA and PC show similar behavior in the quasi-static range. As has been observed in the work of Arruda et al. (1995), their response usually consists of three regimes: an initial linear portion, a yielding and strain softening portion, and, finally, a non-linear strain hardening portion. Rate sensitivity is obvious in both materials. The yield stress for both PC and PMMA at $\dot{\varepsilon} = 0.04$ s^{-1} is higher than that at $\dot{\varepsilon} = 4 \times 10^{-5}$ s^{-1}. For the case of PC, after a certain strain level, the stress of the higher rate test drops below that of the lower strain rate test. Arruda et al. (1995) have explained this phenomenon as being the result of thermal softening present in PC.

Dynamic tests were conducted on the SHPB at strain rates from 400 to 2500 s^{-1}. Original signals from the SHPB for a typical PC test are shown in Fig. 4. Unlike the situation in the Instron machine test, in the SHPB case the value of maximum strain that can be reached depends not only on the material properties, but also on the duration of the loading pulse. (Since typically the PC specimens do not fail catastrophically in the SHPB tests.) The longest loading pulse duration (determined by the projectile length) used in this study was 160 μs. In most cases, enough information can be extracted within this duration. In Fig. 4 note that the two temperature signals are very close to each other for most of the deformation. This indicates that the thermal fields in the specimen are homogeneous throughout the experiment. Also recall that the specimen is in motion in front of the detectors as the experiment progresses. However, from one dimensional wave propagation it is easy to estimate that in the time window recorded, the specimen will have moved approximately only by at most 1 mm. This realization reinforces the fact that the thermal field on the surface is indeed homogeneous.

Mechanical homogeneity can be experimentally verified by comparing the forces at the incident bar/specimen and specimen/transmitted bar interfaces. A typical force record for the case of PC is shown in Fig. 5(a) and for PMMA in Fig. 5(b). Quantities $F_i(= \varepsilon_i EA)$ denotes the incident force in the bar, $-F_r(= \varepsilon_r EA)$ the reflected force, and $F_t(= \varepsilon_t EA)$ the transmitted force. $F_i + F_r$ represents the total force on the incident bar/specimen interface; F_t is the total force on the specimen/reflected bar interface. As can be seen, homogeneity in the SHPB specimen is achieved after a short time. This has been analytically shown to be about four reflections of the wave travelling in the specimen (Ravichandran and Subhash, 1994) although in

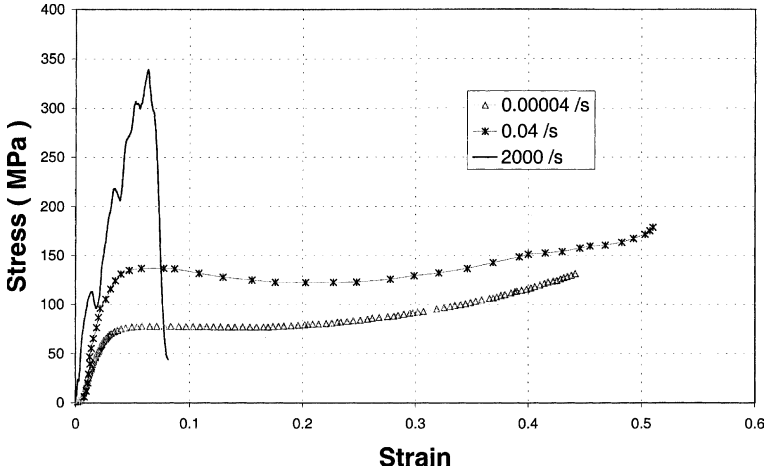

Fig. 2. Compressive stress–strain curves for PMMA at strain rates 4×10^{-5}, 0.04 and 2000 s^{-1}.

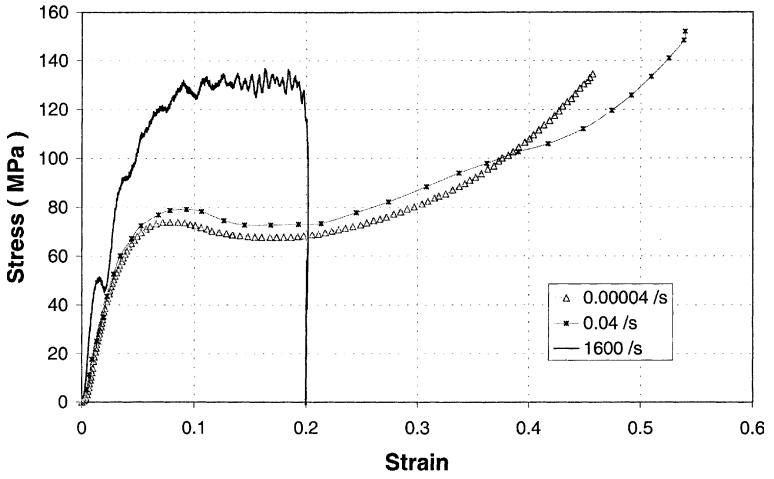

Fig. 3. Compressive stress–strain curves for PC at strain rates 4×10^{-5}, 0.04 and 1600 s^{-1}.

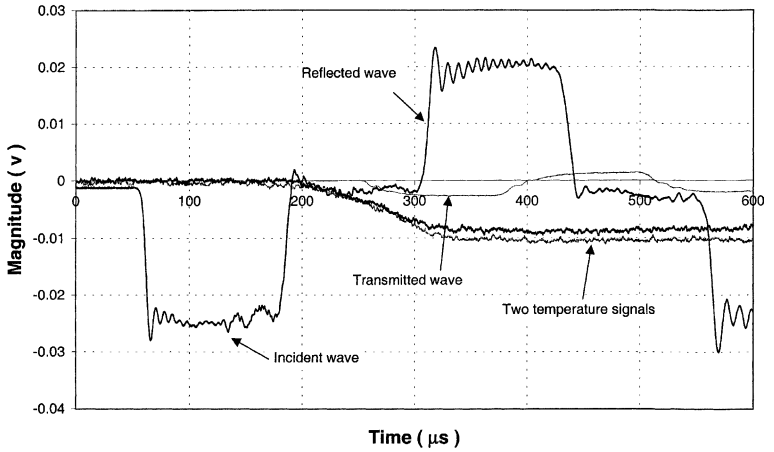

Fig. 4. Original signals from dynamic experiment for PC showing the SHPB response and IR detector signals (two detector signals shown).

some cases equilibrium may be achieved earlier (Gary III and Blumenthal, 1999) depending on the relative acoustic impedance of specimen and bar. Here, the experimental times for homogeneity are found to be about 22 μs for PC and 30 μs for PMMA both well before yield or failure occurs.

A number of dynamic stress–strain curves for PMMA and PC are shown in Figs. 6 and 7, respectively. For comparison with the quasi-static results, one dynamic stress–strain curve for each material has also been plotted in Figs. 2 and 3. It can be seen that the dynamic response shows a continuing rate dependence for both materials in the dynamic strain rate regime.

In dynamic tests, both polymers show an initial linear response followed by what appears to be localized yielding. (Note, however, that many of the subsequent ripples present in the stress–strain curves are from the fluctuations of the loading pulse, shown in Fig. 4, which cannot be eliminated from the experiment.) The main feature of the dynamic PC stress–strain curves is that after yielding occurs a clear non-linear

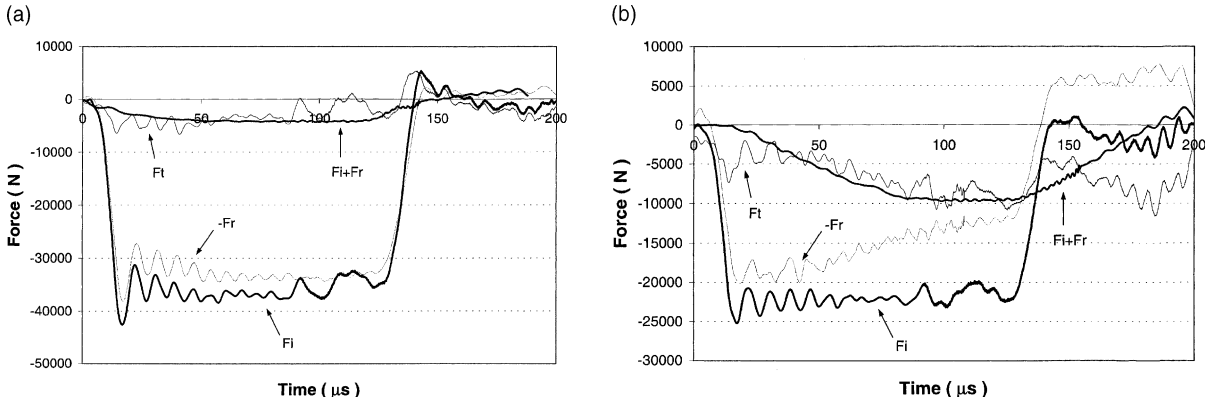

Fig. 5. (a) Force balance for PC during SHPB experiment and (b) Force balance for PMMA during SHPB experiment.

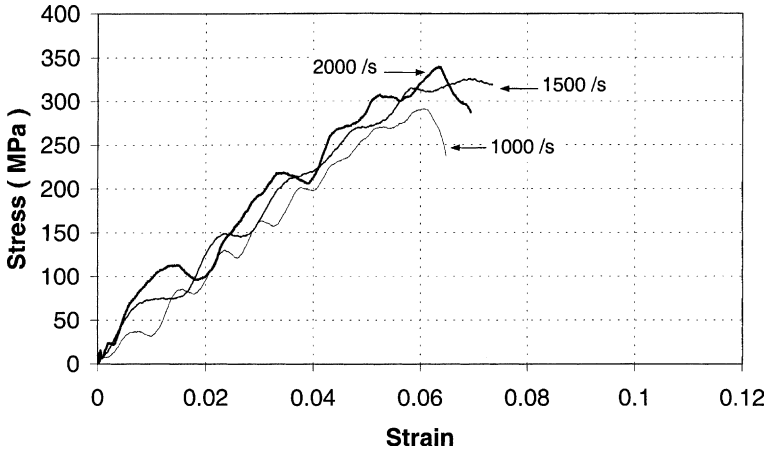

Fig. 6. Dynamic compressive stress–strain curves for PMMA.

plastic deformation regime exists, until specimen unloading. The reason for the final drop of stress in the curves of Fig. 7 and the 1600 s^{-1} curve in Fig. 3, is not specimen failure, but specimen unloading. Examination of the specimens after impact shows that PC specimen is still intact but with significant residual strain. Thus, the response of PC, although certainly rate sensitive, maintains its general characteristics over a large range of strain rates.

In contrast to PC, the dynamic response for PMMA (Fig. 6 and the 2000 s^{-1} curve in Fig. 2) does not exhibit a pronounced non-linear regime. While ripples in the dynamic PMMA stress strain curves do exist and may represent some localized shear yielding or failure, the stress increases to its maximum value in a generally linear fashion and suddenly drops to zero. This occurs considerably before the end of the applied loading pulse and corresponds to actual specimen failure. In fact, the PMMA specimens shatter completely from the impact event. Thus, there is a substantial difference in the response of PMMA over the strain rate range tested. This is best illustrated in the plots of Fig. 2.

By performing experiments at different strain rates, an attempt was made to determine the threshold strain rate for which PMMA would shatter, thus distinctly changing its mechanical response from ductile to

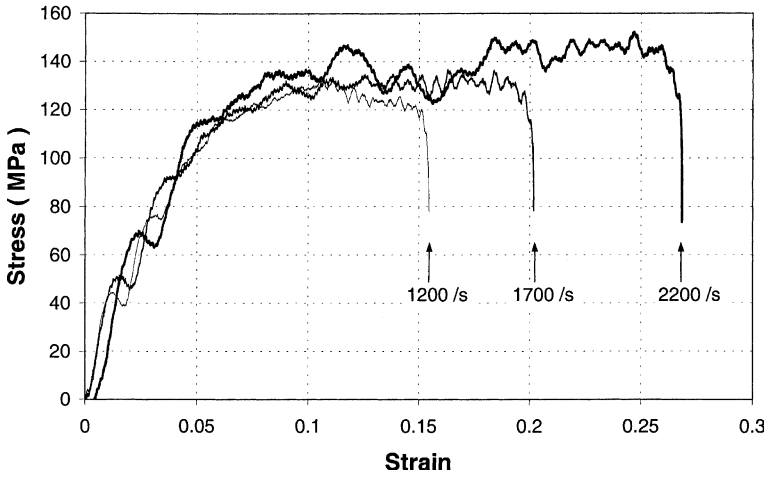

Fig. 7. Dynamic compressive stress–strain curves for PC.

brittle. This threshold level was found to be about 1000 s^{-1} as can be seen in Fig. 8. The stress–strain curves and associated strain rate for two nominally identical tests, labeled as 1 and 2, are shown in this figure. Both specimens were loaded at the same strain rate. After the experiment, the specimen from Test 1 remained intact, while the one from Test 2 shattered. This different response is clearly reflected on the two stress–strain and strain rate–strain curves. In Test 2, stress drops suddenly after it (linearly) reaches a peak value. This corresponds to specimen failure. However, at essentially the same strain rate, the response of Test 1, shows yielding and a distinct non-linear region until the point of specimen unloading not from failure, but from unloading of the external applied strain rate. Thus, the strain rate of approximately 1000 s^{-1} seems to be the "transitional" strain rate for the response of PMMA.

The rate sensitivity of mechanical properties of these materials can be obtained from the stress–strain curves described in this section. The results are summarized in Table 1 for PMMA and Table 2 for PC. Compressive yield stress for both polymers, defined as the first deviation from a linear material response, is

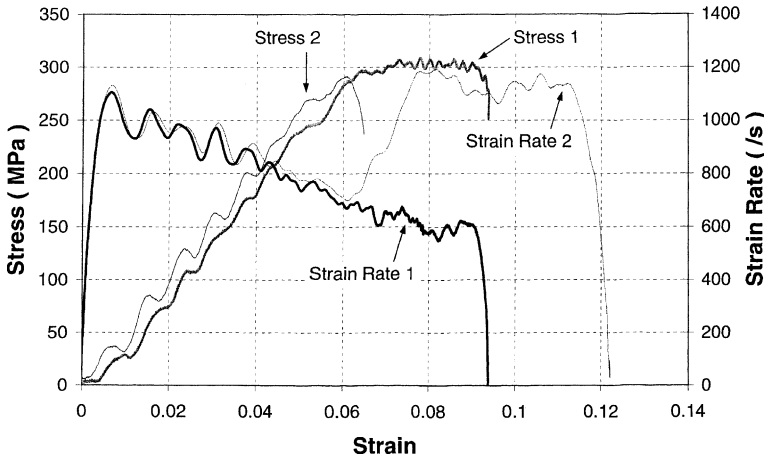

Fig. 8. Two compressive stress–strain and strain rate–strain plots illustrating "transition" behavior of PMMA. Test 2 (~1000 s^{-1}) fractures at a strain of 0.06, unlike Test 1 (also ~1000 s^{-1}) does not fracture at all.

Table 1
Strain rate sensitivity of mechanical properties of PMMA

$\dot{\varepsilon}$ (s^{-1})	σ_y (MPa)	σ_f (MPa)	E (GPa)
0.00004	27.9	N/A	3.4
0.04	32.7	N/A	6.3
1000	37	2910	8.5
1500	75.2	3230	11.5
2000	113	3330	17.0

Table 2
Strain rate sensitivity of mechanical properties of PC

$\dot{\varepsilon}$ (s^{-1})	σ_y (MPa)	E (GPa)
0.00004	25.2	2.4
0.04	35	2.4
1200	47.5	5.4
1700	54.1	5.4
2200	68.9	5.4

seen to vary with strain rate. Modulus of elasticity, obtained from a line fit to this initial linear part of the curve, is also seen to be strain rate dependent. Note, however, that the dynamic results (i.e. for strain rates 1000 s^{-1} and over) for modulus must be taken with some caution since they are obtained from data very close to the time of non-homogeneous deformation in the SHPB experiments. Finally, for the case of PMMA, we also see a mild strain rate sensitivity of the ultimate compressive stress (for strain rates in which global catastrophic failure occurs).

5. Thermal response

As mentioned earlier, temperature measurement was only conducted during the dynamic tests. An investigation of heat generation during quasi-static loading of PMMA has been performed by Arruda et al. (1995). Their results showed that in fact experiments at even a strain rate of 0.001 s^{-1} cannot be considered isothermal. For strain rates exceeding 5000 s^{-1} Rittel (1999) has recently used an embedded thermocouple technique to obtain the temperature at a single point of the interior of a specimen. The present results use an IR detector array that provides a faster rise time than thermocouples and also allows for multiple point recording. However, the IR system can only provide surface temperature measurements, so a direct comparison with the results of Rittel is not possible.

Temperature signals at two locations 1.6 mm apart were recorded in each experiment. An example of the signals obtained from the two detector elements was shown in Fig. 4. Because the output of the IR detectors is always in the form of voltage, a calibration between output voltage and temperature has to be established. In theory, an explicit relation between the detector voltage measurement and the actual temperature can be found, if the emissivity of the surface is known (Zehnder and Rosakis, 1993). Unfortunately, such a relation is not easy to establish because the specimen's emissivity and the detector's spectral responsivity are very difficult to measure. Therefore, an experimental calibration was carried out instead. Temperature was measured independently using a K-type (Chromel–Alumel junction) thermocouple. Before calibration, a thermocouple was inserted into a small hole drilled on the lateral surface of the specimen as close as possible to the opposite lateral surface. The hole was filled with a ceramic cement (OMEGABOND 400 from OMEGA Engineering Inc.). The specimen was then heated in a furnace to a temperature above the

expected maximum temperature of the actual tests, and then inserted in the SHPB. As the specimen cooled to room temperature the voltage reading from the detector was related to the actual temperature reading from the thermocouple, thus providing a calibration curve. A typical calibration curve for a PC specimen is shown in Fig. 9. Curve fitting shows that the relation between the temperature and the voltage is usually a second order polynomial. Since the surface texture of the specimen affects emissivity, it is important to maintain the same specimen preparation technique throughout all experimentation.

It must be pointed out that several factors can affect specimen emissitivity, and thus potentially distort the calibration results. Since the specimen has a curved surface, emissitivity may be affected by surface angle. However, for non-conducting materials this effect is negligible (Incropera and Dewitt, 1981). In addition radiation from material below the surface may reach the detectors. The amount of such sub-surface radiation reaching the detectors is proportional to the transmissivity of the specimen. In general transmissivity depends on wavelength. For the case of PMMA, transmissivity is almost zero in the IR wavelength range in which our detectors are sensitive (Incropera and Dewitt, 1981). No data in this respect are readily available for PC, but the effect is believed to be similar to PMMA. Emissitivity may also vary with temperature, but such a variation would be accounted for in the calibration procedure used here.

Fig. 10 shows the stress–strain curve for PC at a rate of 2200 s^{-1} as well as the temperature signals obtained by two detectors. Note that since temperature is recorded at the specimen location, and the incident and transmitted SHPB signals are recorded away from the specimen, the three signals will not be time coincident. This is clearly seen in the raw signals of Fig. 4. Using wave propagation results in the bars, the temperature and stress–strain curves can be shifted to be time coincident. This has been done in the results shown in Fig. 10 (as well as Figs. 12 and 13). The point (0,0) for both stress and temperature signals, corresponds to the instant of arrival of the loading wave at the incident bar/specimen interface. It is clear from the results of Fig. 10 that temperature in the PC specimen does not show a significant rise until the yield point (around 70 MPa in this case) has been reached. Subsequent to yielding a significant temperature increase of about 5–6° is seen in both detectors. After unloading (not shown in the figure because strain cannot be defined) the temperature stays approximately constant (Fig. 4) denoting that an assumption of adiabatic conditions is not unreasonable at this rate and for this material.

Note that at a certain strain level (e.g. approximate 0.125 for the 2200 s^{-1} curve in Fig. 10) the stress–strain curve for PC seems to exhibit a mild softening behavior. This behavior has also been observed in Rittel (1999), where it was argued that a corresponding increase in temperature shows that this is the region

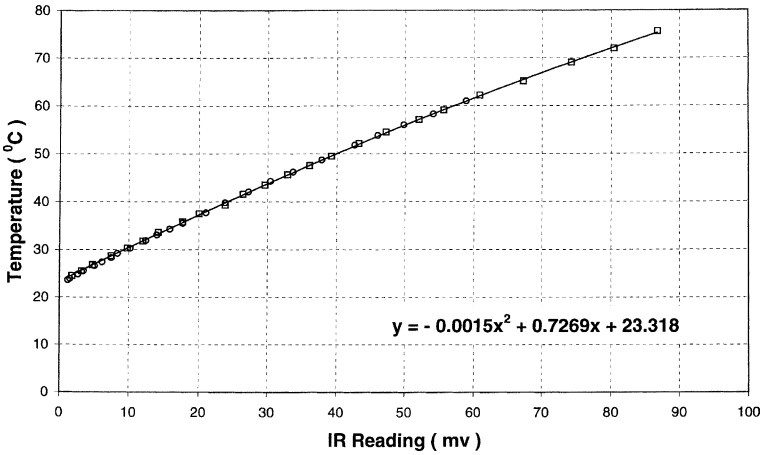

Fig. 9. Typical IR detector temperature calibration curve for PC.

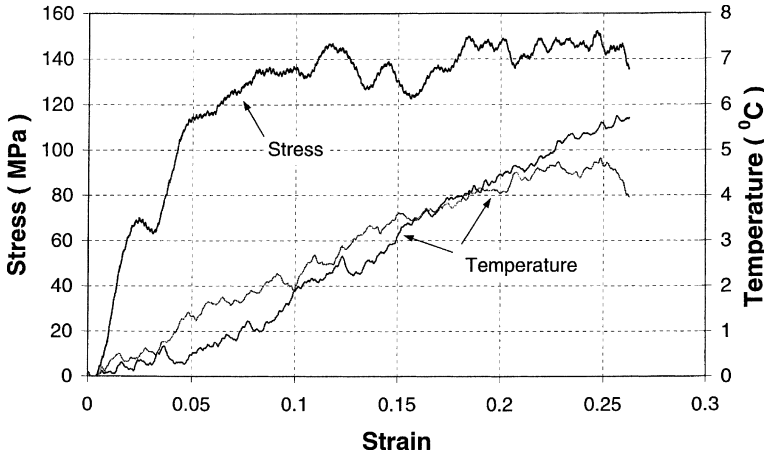

Fig. 10. Compressive stress and temperature vs. strain for PC at a strain rate of 2200 s^{-1}.

where thermal softening overtakes strain hardening. In the present experiments, this effect is not as pronounced since the strain rate employed is much smaller (2200 s^{-1} as opposed to approximate 6500 s^{-1} in the work of Rittel). In general, however, the thermomechanical response of PC is similar to that of ductile metals (Mason et al., 1994; Hodowany et al., 2000) in which there is no obvious temperature change during the initial elastic deformation stage, and temperature starts rising once plastic deformation occurs. Thus, concepts and models, established for metals should be useful for the dynamic response of PC.

An attempt to extend existing thermomechanical models for metals (Mason et al., 1994; Hodowany et al., 2000) is currently being made. The starting point for this attempt is the evaluation of the amount of plastic work converted to heat, β, presented in Eqs. (3) and (4). Since an independent measurement of temperature (from the IR detectors) and plastic work (from the stress–strain curve) can be made, it is possible to use these two equations to obtain values for β. This can be done for various strain levels within each experiment and for various strain rates between different experiments. As has been pointed out by Rittel (1999), an integral and a differential form of β can be defined. Evaluating the differential form involves differentiation of discrete experimental data and will thus contain a higher amount of error than the integral form.

Values of β for PC are plotted against strain in Fig. 11 for strain rates of 1200, 1700 and 2200 s^{-1}. Only the integral form of β is shown. It can be seen that β_{int} shows a strain sensitivity for low values of strain, and it decreases as strain increases. This strain sensitivity region corresponds to the transition region connecting the initial yield point and the plateau on the stress–strain curve. Once the stress reaches the plateau, β_{int} also plateaus at a value of 0.5. These values are in general agreement with the quasi-static result of Adam and Farris (1988), approximately 0.5–0.8. Rittel (1999) β_{int} at strain rates beyond 5000 s^{-1} is in the range of 0.4 to 1, but it has a somewhat stronger rate sensitivity as strain rate increases. However, it must be kept in mind that the measurements of Rittel were performed in the interior of the specimen and at much higher strain rates (5000–8000 s^{-1}). As mentioned above, obtaining β_{diff} requires calculation of $\dot{T}$, i.e., numerical differentiation of the noisy temperature signals. This can lead to significant error. One way to bypass this problem is to curve-fit the temperature versus time data and take the derivative from the resulting equation. However, results for β_{diff} are unreliable, even using a curve fitting type of approach and will not be shown here.

For the case of PMMA loaded below the threshold strain rate of 1000 s^{-1}, a slight temperature increase of about 1 to 2°C is observed (Fig. 12). For strain rates beyond 1000 s^{-1} (Fig. 13), a different thermal

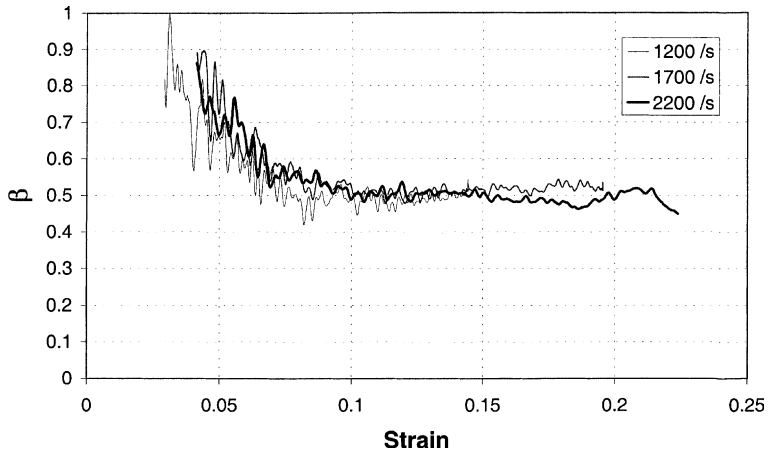

Fig. 11. β_{int} vs. strain at different strain rates for PC.

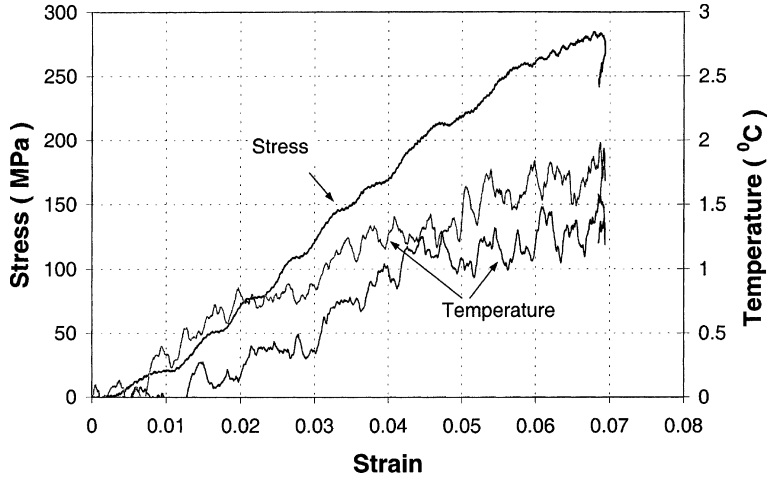

Fig. 12. Compressive stress and temperature vs. strain for PMMA at a strain rate of 800 s^{-1}.

behavior is observed. In the loading portion of the event, both stress and temperature behave exactly as those at lower strain rates. However, once the material fails, which is signified by the sudden drop of stress, the temperature undergoes a significant and abrupt increase. In the present experiments, however, we can see that the signals from the spatially separated detectors are similar to each other until failure occurs, after which point they deviate considerably. This suggests a widely non-homogeneous failure, which is consistent with fragmentation of the specimen. Other polymeric materials that undergo similar fragmentation exhibit this sudden temperature increase. An example can be found in the experiments performed by Trojanowski et al. (1997) on the epoxy resins. The implication of this observation is that a portion of the work input into the PMMA specimen is converted to heat at the instant of failure. This suggests that in a fracture situation PMMA is not perfectly brittle since some thermal energy is required (in addition to Griffith surface energy for creation of new surfaces). The thermal response during dynamic fracture experiments in PMMA is investigated in a complementary study by Bjerke and Lambros (2000).

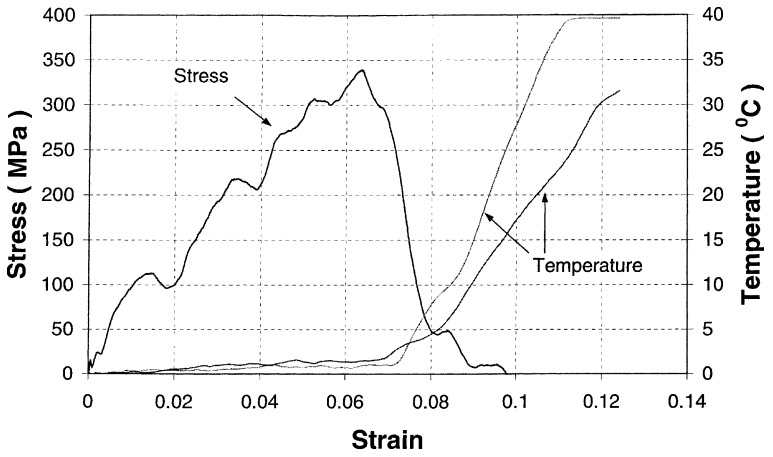

Fig. 13. Compressive stress and temperature vs. strain for PMMA at a strain rate of 2000 s^{-1}.

6. Conclusions

Thermomechanical strain rate sensitivity of two common polymers, PMMA and polycarbonate, subjected to compressive loading was investigated in this paper. Stress–strain response was examined over a wide range of strain rates, from 10^{-4} to 10^{3} s^{-1}. For PMMA, the material changes its behavior from ductile to brittle as compressive strain rate increases. The threshold strain rate for such a transition was found to be about 1000 s^{-1}. Although a minor temperature increase ($\sim$1 to 2°C) was observed during loading of PMMA, β in this material cannot be, strictly speaking, defined. For PC, it is found that yield stress increases as strain rate increases. In addition, the competition between thermal softening and strain hardening dictates the behavior after yielding. As strain rate increases, adiabatic heating caused by high speed loading enables thermal softening to prevail in the competition, causing the slope of strain hardening drop. Measurement of β was performed for PC. The integral form of β was found to be within the range of 0.5–0.6 for the strain rates ranged from 400–2500 s^{-1}. Although there is a weak strain dependency for β, no strain rate dependency was observed in this strain rate range.

Acknowledgements

The support of NSF (grant numbers CMS-9712291, CMS-9622241) for this work is gratefully appreciated. We also wish to thank Mr. Jeremy Freeman for his assistance with some of the experimentation.

References

Adams, G.W., Farris, R.J., 1988. Latent energy of deformation of bishenol a polycarbonate. Polymer Engineering and Science Part B Polymer Physics 26, 433–445.

Arruda, E.M., Boyce, M.C., Jayachandran, R., 1995. Effects of strain rate, temperature and thermomechanical coupling on the finite strain deformation of glassy polymers. Mechanics of Materials 19, 193–212.

Bjerke, T.W., Lambros, J., 2000. Thermomechanical behavior of polymers during opening and shear dominating dynamic fracture, submitted for publication.

Boyce, M.C., Arruda,, E.M., Jayachandran, R., 1994. The large strain compression, tension and simple shear of polycarbonate. Polymer Engineering and Science 34 (9), 716–725.

Boyce, M.C., Montagut, E.L., Argon, A.S., 1992. The effects of thermomechanical coupling on the cold drawing process of glassy polymers. Polymer Engineering and Science 32 (16), 1073–1085.

Chou, S.C., Robertson, K.D., Rainey, J.H., 1973. The effect of strain rate and heat developed during deformation on the stress–strain curve of plastics. Experimental Mechanics 13 (3), 422–432.

Farren, W.S., Taylor, G.I., 1925. The heat developed during plastic extension of metals. Proc. R. Soc. CVII, 422-451.

Follansbee, P.S., 1985. High strain rate compression testing, Mechanical Testing Volume, ASM Handbook, ninth ed. vol. 8, pp. 198–203.

Gary III, G.T., Blumenthal, W.R., 1999. Split Hopkinson Pressure Bar testing of soft materials. Rep. No. LA-UR-99-4878, Los Alamos National Laboratory.

Hodowany, J., Ravichandran, G., Rosakis, A.J., Rosakis, P., 2000. Partition of plastic work into heat and stored energy in metals, Experimental Mechanics 40 (2), 113–123.

Incropera, F.P., Dewitt, D.P., 1981. Fundamentals of Heat Transfer, Wiley, New York.

Kapoor, R., Nemat-Nasser, S., 1998. Determination of temperature rise during high strain rate deformation. Mechanics of Materials 27, 1–12.

Li, Z., Lambros, J., 1999. Determination of the dynamic response of brittle polymeric matrix composites using the split Hopkinson pressure bar. Composite Science and Technology 59, 1097–1107.

Mason, J.J., Rosakis, A.J., Ravichandran, G., 1994. On the strain and strain rate dependence of the fraction of plastic work converted into heat: an experimental study using high speed infrared detectors and the Kolsky bar. Mechanics of Materials 17, 135–145.

Ravichandran, G., Subhash, G., 1994. Critical appraisal of limiting strain rates for compression testing ceramics in a split hopkinson pressure. Journal American Ceramic Society 77, 263–267.

Rittel, D., 1999. On the conversion of plastic work to heat during high strain rate deformation of glassy polymers. Mechanics of Materials 31, 131–139.

Taylor, G.I., Quinney, H., 1934. The latent energy remaining in a metal after cold working. Proc. Roy. Soc. Ser. A 143, 307–326.

Trojanowski, A., Ruiz, C., Harding, J., 1997. Thermomechanical properties of polymers at high rates of strain. Journal of Physics. IV France 7, C3.

Walley, S.M., Field, J.E., Pope, P.H., Safford, N.A., 1989. A study of the rapid deformation behavior of a range of polymers. Philosophy Transactions Society London A 328, 783–811.

Zehnder, A.T., Rosakis A.J., 1993. Temperature rise at the tip of dynamically propagating cracks: measurements using high-speed infrared detectors. Chapter 5: Experimental Techniques in Fracture, VCH Publishers.